Published in final edited form as:
Int J Dev Neurosci. 2011 December ; 29(8): 847–854. doi:10.1016/j.ijdevneu.2011.08.002.

Developmental Differences in Peripheral Glabrous Skin Mechanosensory Nerve Receptive Field and Intracellular Electrophysiologic Properties: Phenotypic Characterization in Infant and Juvenile Rats

M. Danilo Boada, MSc, PhD[a], **Silvia Gutierrez, PhD**[b], **Timothy Houle, PhD**[c], **James C. Eisenach, MD**[d], and **Douglas G. Ririe, MD, PhD**[e]
Department of Anesthesiology, Wake Forest School of Medicine, Winston-Salem, North Carolina, USA

[a] Research Assistant Professor of Anesthesiology (mboada@wakehealth.edu)

[b] Research Postdoctoral Fellow (sgutierr@wakehealth.edu)

[c] Associate Professor of Anesthesiology (thoule@wakehealth.edu)

[d] Professor of Anesthesiology (eisenach@wakehealth.edu)

[e] Associate Professor of Anesthesiology (dririe@wakehealth.edu)

Abstract

Developmental differences in peripheral neuron characteristics and functionality exist. Direct measurement of active and passive electrophysiologic and receptive field characteristics of single mechanosensitive neurons in glabrous skin was performed and phenotypic characterization of fiber subtypes was applied to analyze developmental differences in peripheral mechanosensitive afferents. After Institutional approval, male Sprague-Dawley infant (P7: postnatal day 7) and juvenile (P28) rats were anesthetized and single cell intracellular electrophysiology was performed in the dorsal root ganglion (DRG) soma of mechanosensitive cells with receptive field (RF) in the glabrous skin of the hindpaw. Passive and active electrical properties of the cells and RF size and characteristics determined. Fiber subtype classification was performed and developmental differences in fiber subtype properties analyzed. RF size was smaller at P7 for both low and high threshold mechanoreceptor (LTMR and HTMR) with no differences between A- and C-HTMR (AHTMR and CHTMR). The RF size was also correlated to anatomic location on glabrous skin, toes having smaller RF. Conduction velocity (CV) was adequate at P28 for AHTMR and CHTMR classification, but not at P7. Only width of the action potential at half height (D50) was significantly different between HTMR at P7, while D50, CV and Amplitude of the AP were significant for HTMR at P28. RF size is determined in part by the RF distribution of the peripheral neuron. Developmental differences in RF size occur with larger RF sizes occurring in younger animals. This is consistent with RF size differences determined by measuring RF in the spinal cord, except the peripheral RF is much smaller, more refined, and in some cases pinpoint. Developmental differences make CV alone unreliable for neuron classification. Utilizing

Address correspondence to: Dr. Boada, Department of Anesthesiology, Wake Forest School of Medicine, Medical Center Boulevard, Winston-Salem, NC 27157-1009 Phone: 336-716-4498 Fax: 336-716-8190 dboada@wakehealth.edu.

integration of all measured parameters allows classification of neurons into subtypes even at the younger ages. This will prove important in understanding changes that occur in the peripheral sensory afferents in the face of ongoing development and injury early in life.

Keywords

development; electrophysiology; peripheral nerve; postnatal; receptive field

1. Introduction

At birth completely novel stimuli begin to activate peripheral sensory neurons and stimulate changes that lead to the adult sensory phenotype. The specific sensory phenotype seems to be target specific (Boada et al., 2010; Lu et al., 2001). This culminates in functional sensory integration from the peripheral neuron to the spinal cord and brain that is anatomically discrete. The changes in the periphery have functional consequences that allow accurate coding of information. This appears to be critical for proper organization of higher centers and the resulting appropriate behavioral responses (Fitzgerald, 1985; Rowe, 1982). Many of the neuronal changes have been defined in the developing rat leading to a conceptual framework for understanding somatosensory maturation.

It appears that all the elements of the adult peripheral sensory nervous system are present at birth (Fitzgerald, 1985). This includes the full complement of mechanosensory neurons. However, the phenotypes of mechanosensory neurons are immature at birth. Developmental increases in conduction velocity (CV) and stimulus response characteristics occur during the first several weeks postnatally (Fitzgerald, 1985; Fulton, 1987; Fitzgerald, 1987). In addition, the linkage of the different sensory fibers to second order neurons in the spinal cord is developmentally regulated (Fitzgerald, 1988). This has been best defined with the inability of c-fibers to activate second order neurons in the spinal cord completely until the second postnatal week, despite the fact that these peripheral neuronal responses are fully functional at birth (Fitzgerald and Gibson, 1984; Fitzgerald, 1988).

Since injury can and does occur during this critical period of development, the responses of all peripheral nerve fibers are valuable in understanding short and long term effects of the injury on neuronal processing of the injury centrally (Li et al., 2009; Ririe et al., 2008). In particular, understanding how information is coded and conveyed from the periphery during the developmental period prior to the establishment of functional connections of c-fibers will be important in understanding the effects of nociceptive or noxious stimuli at this time. A-fibers may assume a different role in transmission of information to the spinal cord to accommodate for the dysfunctional c-fibers. It is entirely plausible that the fast conducting fibers (both low threshold mechanoreceptors [LTMRs] and A-high threshold mechanoreceptors [AHTMRs]) that deeply invade the neonatal dorsal horn (DH) superficial laminae transmit information reserved for c-fibers later in development (Coggeshall et al., 1996; Fitzgerald et al., 1994). Neuronal plasticity makes the neonatal DH potentially susceptible to “remodeling” by changes in peripheral inputs, particularly on areas of conversion for fast afferents, such as the substantia gelatinosa (SG) (Li and Baccei, 2009; Woolf and Fitzgerald, 1983). Since the postnatal sensory experience is a driving force for the development of normal DH architecture and functional sensory pathways, the comparison between naïve states of these afferents and their intermediate juvenile characteristics become relevant (Beggs et al., 2002).

Conduction velocity has been used to classify neurons, but CV is rapidly changing during early development (Lawson 2002; Harper and Lawson, 1985; Fitzgerald, 1987). Significant

changes in CV of the “fast” fibers result from changes in myelination (Friede and Samorajski, 1968). The combination of conduction velocity and mechanical properties has been used to sub-classify HTMR as medium and slow conducting fibers (A/C), Aδ nociceptors (AHTMR) and C-nociceptors (CHTMR) (Campbell et al. 1989; Bessou and Perl 1969; Light and Perl 1993; Lawson 2002; Albers et al. 2006). This assumed that tactile afferents (LTMR) were fast conducting fibers (Aβ/Aδ) (Perl 1992), but slower tactile afferents (Aδ/C) (Burgess and Perl 1967; Boada and Woodbury 2007, 2008) and fast-nociceptors (Aβ) (in addition to the Aδ-nociceptors) have been reported (Light and Perl 1993; Woodbury and Koerber 2003; Boada and Woodbury 2007). This renders utilization of more physiologic parameters to sub-classify sensory neurons useful even in the mature animal. More importantly, the mechanosensitive responses early in development have not reached the level attained later in maturity. Thus in order to examine and understand developmental differences in physiologic characteristics of neuronal populations, accurate classification of neuron subtypes is critical. This will permit understanding the changing roles and responses of the nerve fiber subtypes independent of CV at baseline early in development will allow studies of the impact of injury both in the peripheral nerves and in the DH. This is of particular interest since differences in timing of arrival of neuronal signals from changing CV during development and as a result of injury may have profound and lasting effects.

The objective of the current study is to provide key knowledge about the initial naïve state of these peripheral sensory nerve fibers at discrete ages during development in their most natural environment. We have focused on direct intracellular electrophysiologic comparisons of intact mechanosensory fiber subtype receptive fields (RFs) and characteristics. We utilized these properties to phenotypically characterize neuronal subtypes when CV is rapidly changing. Establishing these fundamental data in neurons from glabrous skin will allow studies to understand noxious input or injury and the effects on peripheral sensory transmission and neuronal CV and character, which could contribute to neuropathological conditions both acutely and in later life.

2. Materials and Methods

After Institutional Animal Care and Use Committee approval, male Sprague-Dawley infant (postnatal day 7) and juvenile (postnatal day 28) rats were deeply anesthetized with isoflurane 3% with spontaneous ventilation. The trachea was intubated and animals ventilated using pressure controlled ventilation (Inspira PCV, Harvard Apparatus, Holliston, MA, USA) with humidified oxygen. The ECG was monitored throughout. Anesthetized animals were immobilized with pancuronium bromide and the isoflurane maintained at 2% throughout the study (Tevan Pharmaceutics, North Wales, PA, USA). As illustrated in Figure 1, a dorsal midline incision was made in trunk skin and L5 DRG and adjacent spinal cord was exposed by laminectomy as previously (Boada et al., 2010). The tissue was continuously superfused with oxygenated artificial cerebrospinal fluid [aCSF (in mM): 127.0 NaCl, 1.9 KCl, 1.2 KH2PO4, 1.3 MgSO4, 2.4 CaCl2, 26.0 NaHCO3, and 10.0 D-glucose]. The spinal column was secured using custom clamps and the preparation was transferred to a preheated (32-34°C) recording chamber where the superfusate was slowly raised to 37°C (MPRE8, Cell MicroControls, Norfolk, VA, USA). Pool temperature adjacent to the DRG was monitored with a thermocouple (IT-23, Physitemp, Clifton, NJ, USA). Rectal temperature (RET-3, Physitemp) was maintained at 34 ± 1°C with radiant heat.

DRG soma were impaled with borosilicate microelectrodes (80-250 MΩ) containing 1 M potassium acetate (in some cases also 20% neurobiotin (Vector Laboratories, Burlingame, CA, USA)). Intracellular penetrations with a resting membrane potential of ≤ -35 mV were

characterized further. DC output from an Axoclamp 2B (Axon Instruments/Molecular Devices, Sunnyvale, CA, USA) was digitized and analyzed off-line using Spike2 (CED, Cambridge, UK). Sampling rate for intracellular recordings was 21 kHz throughout (MicroPower1401, CED).

After achieving stable cell impalement, the skin was searched with a fine sable-hair brush to locate the peripheral RF. For afferents requiring higher intensities, subsequent searches used increasingly stiffer probes and finally sharp-tipped forceps. Afferents with cutaneous RFs were distinguished from those with deep RFs by displacing skin to ensure that RFs tracked rather than remained stationary. Mechanical thresholds were characterized with calibrated von Frey filaments (Stoelting, Wood Dale, IL, USA). Adaptation rate was frequently evaluated using micromanipulator-based probes; responses to skin stretch and vibratory stimuli were also tested. In all cases, RFs were characterized and measured with the aid of a zoom stereomicroscope.

Active membrane properties of all identified sensory neurons were analyzed including the amplitude and duration of the action potential (AP) and afterhyperpolarization (AHP) of the AP, along with the maximum rates of spike depolarization and repolarization (MRD and MRR); AP and AHP durations were measured at half-amplitude (D50, AHP50) to minimize hyperpolarization-related artifacts. Passive properties were analyzed including membrane resting potential (Em), input resistance (Ri), time constant (Tau), inward rectification, and, where possible, rheobase; all but the latter were determined by injecting incremental hyperpolarizing current pulses (≤ 0.1 nA, 500 ms) through balanced electrodes.

Because intact lumbar DRGs serve multiple nerves, spike latency was obtained by stimulating the RF at the skin surface using a bipolar electrode (0.5 Hz); this was performed following all natural stimulation to prevent potential alterations in RF properties. Because we were interested in latency from terminals, all measurements were obtained using the absolute minimum intensity required to excite neurons consistently without jitter; significantly shorter latencies, seen at traditional (i.e., two- to three-fold threshold) intensities and presumably reflecting spread to more proximal sites along axons. Any neuron with jitter was rejected. Stimuli ranged in duration from 50 to 100 μs; utilization time was not taken into account. Conduction distances were measured for each afferent on termination of the experiment by inserting a pin through the RF (marked with ink at the time of recording) and carefully measuring the distance to the DRG along the closest nerve.

All included cells satisfied the following requirements: resting membrane potential more negative than -30 mV, AP amplitude ≥30 mV and the presence of spike AHP. Passive membrane properties indicative of poor impalement were also reason for exclusion.

2.1 Receptive field (RF) analysis

After establishing the afferent identity, the RF was carefully searched with suprathreshold mechanical stimuli. The force used was equivalent to the group upper limit of their cutoff force (±0.33 mN) for the tactile and for the nociceptive afferents was 9.02 mN unless their threshold was higher in value. The highest force possible without compromise to the cellular impalement was <100.94 mN.

During the glabrous skin RF mapping, different parameters were established: 1) number and location of “spots” with the highest sensibility (lowest threshold responses), 2) absolute RF area (mm^2) at threshold intensity, 3) relative RF area (%) normalized to glabrous skin total foot area for age (P7: 69.2 mm^2, P28: 355.7 mm^2). Specific functional areas (fingers against paw) were both analyzed as independent sectors (P7 fingers (Z1): 27.2 mm^2, P7 Paw (Z2): 42.0 mm^2; P28 fingers (Z1): 109.4 mm^2, P28 Paw (Z2): 246.3 mm^2). All values where

obtained by diagramming the cellular RF to later establish absolute area. The area measurements were performed using StereoInvestigator 7.0 (MicroBrightField Inc, Williston, VT, USA) that was supported by an Olympus BX51 microscope and a digital camera (Microfire A/R, Optronics, Goleta, CA, USA). The perimeter of the drawing represented the RF mapped (contour) at 4× magnification. Stereoinvestigator automatically performed several contour measurements including the area.

2.2 Data Analysis

All data are presented as mean with standard error of the mean, except for mechanical thresholds (MT) which are presented as medians and ranges. Statistical analysis was performed using SAS 9.2, (Cary, NC, USA). Multivariate statistical analysis was used to predict and categorize neurons. Canonical correlation was utilized to determine the relationship between all of the variables and the fiber subtypes. Canonical variates were generated from the measured variables to predict the highest correlation between variable value and fiber type classification in the P28 animals. The goal was to capture the variance in measurements by redistribution into variates which capture a large share of the variance.

The canonical variates were used to classify the neurons in the P28 animals and determine the sensitivity, specificity and positive and negative predictive value for the classification using the model. The means and standard deviations were determined for all neuronal subtypes determined from the classification of neurons into LTMR, AHTMR and the CHTMR from the canonical correlation. ANOVA was performed to test for differences in LTMR and HTMR within age. Except for MT where Kruskall-Wallis was used. Significant differences between AHTMR and CHTMR were determined using a Bonferroni post-test comparison of means. RF area estimations were compared in the paw and fingers normalized RF area mean values among Tactiles and Nociceptors at each age (P7 and P28) by ANOVA. By convention, $P<0.05$ was considered significant.

3. Results

In the present study, a total of 108 physiologically identified and well-characterized dorsal root ganglion (DRG) sensory neurons were recorded intrasomally at lumbar level (L5) *in vivo* and their RF characterized on superficial extremity glabrous skin (foot) of both juvenile (P28, n=29) and neonate (P7, n=51) rats. These cells were classified further using different criteria (see Methods), as tactile (LTMR) (P28 n=31, P7 n= 25), or nociceptive (HTMR) (P28 n= 26; P7= 26) afferents innervating glabrous (P28 n=57; P7 n=51) skin at both animal ages, recorded from 30 P28 (1.9 neurons per preparation) and 12 P7 (4.3 neurons per preparation). Intracellular recordings ranged from 25 to 75 min with a stable resting membrane potential throughout. DRG temperatures were tightly controlled around normal core temperatures (37 ± 0.5°C) (Fig. 1). The tactile sub-group includes both rapid and slow adapting units (LTMR RA and SA); however, this last tactile population (SA) was rarely found (P7 n=2, P28 n= 4).

3.1 Model Development for Neuronal Classification

A model was developed to define peripheral afferent sensory phenotype from the measured physiologic variables. All data from the P28 neurons were subjected to canonical correlation to classify cells based on measured physiologic parameters. This involved 13 variables. Of the 13 variables, 4 were eliminated due to insignificant contribution to the factor weight in the model. These were Ri (input resistance), Tau, MRD and MRR (maximum rate of depolarization and repolarization), and RMP (resting membrane potential).

Two canonical variates were derived for neuronal subtype discrimination. Weighted factors were determined and are presented in Table 1. These were used to calculate the canonical variates using the raw canonical coefficients for each neuron. The canonical variates were used to separate the neurons into low threshold mechanoreceptor (LTMR), A-high TMR (AHTMR) and C-high TMR (CHTMR). The first canonical variate was used to discriminate between the LTMR and the HTMR, termed the Low-High Mechano-Discriminator (LHMD). The second canonical variate was used to discriminate the AHTMR from the CHTMR neurons, termed the A-C Mechano-Discriminator (ACMD).

The first canonical variate, LHMD, classified 25/56 or 45% (95% C.I. 32, 58) neurons as LTMR. This resulted in 100% of the LTMR and HTMR neurons from P28 being classified correctly. This was a result of the heavy weighting of the vibration factor which virtually defines the LTMR by the response to 250 Hz (either rapidly adapting or slowly adapting). The second canonical variate, ACMD, was used to determine the classification of the HTMR into either AHTMR or CHTMR. Any ACMD variate value >1.4 was classified as a CHTMR and any <1.4 as AHTMR. The 3 neuronal subtypes were defined by the 2 canonical variates and are presented in Figure 2. The mean canonical variates were LHMD/ACMD respectively: P28, LTMR=320/-0.004, AHTMR=-268,-0.8, CHTMR -268/2.7 and for P7, LTMR=321/1.7, AHTMR=-268/0.7, and CHTMR=-268/2.52. In P28 7/31 or 23% (95% C.I. 15, 30) of the HTMR were classified as CHTMR. Results of the classification in P28 are presented in Table 2. The sensitivity and specificity of the model in the P28 neurons for classification of AHTMR and CHTMR neurons were 96% and 86%, respectively. The positive and negative predictive values of the model for these neurons in P28 were also 96% and 86%, respectively.

This canonical correlation was then applied to classify the neurons from the P7 animals. The first canonical variate, LHMD, classified 25/51 or 49% (95% C.I. 35, 63) neurons as LTMR. The second canonical variate, ACMD, was then used as previously with a discriminating factor of 1.4 to classify HTMR into CHTMR and AHTMR. In the p7, 5/26 or 19% (95% C.I. 4, 34) of the cells were classified as CHTMR. The rest were classified as AHTMR neurons. This classification was used for all further analysis of differences in physiologic variables between different nerve fiber types at the different ages.

3.2 Developmental differences in afferent RF in glabrous skin

Variations in the normalized RF size exist in the periphery for both P7 and P28 animals (Fig. 3). Representative RF and their responses for both LTMR and HTMR in the glabrous skin of the foot are shown in Figure 3A. The LTMR RF is larger than the HTMR in both P7 and P28 animals. Furthermore, the RF area of the P7 animals is larger for both LTMR and HTMR and is shown in Figure 3B. However, the differences in RF size are not homogenous across the glabrous surface of the foot, but are dependent on the function of the tissues innervated by the afferent. Glabrous skin of afferents innervating the toes at P7 and P28 are smaller than those innervating the sole, except in the case of the adult nociceptive afferents (Fig. 3C). No differences in RF size were found between AHTMR and CHTMR at either age.

There were also differences in the character of the RF between the LTMR and HTMR. At both ages (P7 and P28) LTMR showed a multi-spot RF with 2-3 threshold points (spots were the minimal force required to activate the terminal). However, the HTMR subtype at P28 showed an almost “pinpoint” RF with a single spot of mechanical activation at threshold as well as suprathreshold forces. Surprisingly, at P7 the RF of the HTMR were not only larger than at P28, but also showed a multi-spot configuration (2-3 spots per RF) in more than the 60 % of the cells (Figure 3A).

At the same time that RF size is different with larger relative surface area innervated by skin terminals, there are also profound differences in mechanical threshold (MT). The MT was different for LTMR and HTMR afferents in both P7 and P28 animals (see Table 3). The LTMR had a far lower MT than HTMR at both ages. No differences were observed between the different ages for LTMR or HTMR MT. No differences in MT were present between AHTMR and CHTMR at either age.

3.3 Electrical properties of sensory neurons from glabrous skin during development

While differences in somatic electrical properties for LTMR and HTMR afferents exist for 4/9 somatic electrical properties parameters for the P28, there are differences in only 3/9 for the P7 neurons. When looking at differences in HTMR neurons, differences exist in only 2/8 (AP amplitude and D50) for P28 and only 1/8 (D50) for P7 (Table 3). In P28 neurons, the afferent type was related to CV. However, in neurons from the P7, afferents clustered below the Aβ cutoff (11.8 m/s)) of glabrous skin for adults. At P7, the LTMR had a faster CV than HTMR, but the differentiation of HTMR into AHTMR and CHTMR based solely on CV in the infant is not possible because the difference in CV is not significant (Table 3). As development progresses, the LTMR afferents speed up CV as they reach P28, while the HTMR afferents clearly split into two different groups based on CV. Using CV and then D50 as the second variable heavily weighted in the canonical correlation variate (ACMD), this can be seen graphically (Fig. 4A). This also demonstrates the significant overlap of CV in the P7 neurons and makes clear the inability to discern the different subtypes based on CV alone early in development (P7). While canonical correlation used all variables, the 2 most potent and heavily weighted variables in the canonical correlation variate, ACMD (AP amplitude and D50), allow visualization of the role of CV in the separation of the LTMR and HTMR between P7 and P28 (Fig. 4B).

4. Discussion

In this report we describe both the early (infant) and intermediate (juvenile) characteristics of intact mechanosensory afferents in the L5 dermatome from glabrous skin of the foot and their properties (electrical and peripheral) under normal physiological conditions. Reliable neuronal classification during development has permitted examination and comparisons of neuronal characteristics at different stages of growth and provided a fundamental understanding of peripheral sensory processing of neuronal subtypes in the young.

The cornerstones of physiologic classification of sensory neurons are based on conduction velocity, mechanical response, and action potential characteristics. During development significant changes in these parameters during growth and maturation render criteria used in the mature animal less reliable. Comparison of LTMR and HTMR neurons during development demonstrates that after birth a critical time period exists for the normal maturation process in the peripheral mechanosensitive afferent neurons. Both afferent subtypes increase CV passing from a slow conducting fiber cluster (Aδ-C) to a typical two-cluster configuration (Aβ-Aδ and C) in the glabrous skin (Boada et al., 2010). The mean duration of the somatic action potentials was found previously to be characteristic for each of the CV fiber type groupings (Djouhri et al., 1998; Harper and Lawson, 1985a, 1985b). This was also a valuable property in our study (D50) that held up during age, but there was no cutoff and overlap did occur as with CV. Differences in AHP described previously between HTMR and LTMR were also consistent over age, but did not seem to be developmentally different nor play a role in discriminating AHTMR from CHTMR afferents. Despite this, combining all parameters in the canonical correlation proved powerful to separate afferent subtypes.

The process of increasing CV is consistent with simultaneous changes of somatic electrical properties, most likely reflecting increments in fiber myelinization and somatic size as previously described by different authors (Friede and Samorajski, 1968; Fitzgerald, 1985; Fitzgerald, 1987). Increasing separation of fiber subtype from CV alone as development progresses may occur through: no myelination and increasing length as the animal grows and a decrease in CV, b. increase in myelination and increase in length to keep the CV the same (fast or slow), or c. increase in myelination out of proportion to the increase in length to result in increase in CV. Most likely all of these play a role in CV changes during development.

There are data to suggest that electrical activity alters myelination and sodium channel expression and may play a role in plasticity (Klein et al., 2003). Changes in CV and further separation of neurons during development based on electrophysiologic properties may be related to differences in expression of the NaV1.9 channels, with a larger number of Abeta neurons containing NaV1.9 earlier in development (Benn et al., 2001). This may alter AP duration and height of the AP between the different afferent nerve types, which could be altered from injury and result in phenotypic switching (Fang et al., 2005). Although it is plausible that the populations may undergo modality switching in response to injury early in development, it seems likely that the mechanosensory neuronal properties are established early in postnatal life, but studies of injury early in life will determine the ability to alter phenotype.

By combining all the data, a more powerful classification regimen stands up to changes early in development. This is the first report to our knowledge that uses all of the electrophysiologic data from DRG neurons with variable weighting and canonical correlation to classify neurons at different stages of development. The ability to characterize these neurons is particularly important because it implies that function and physiologic properties of mechanosensitive populations are established (tactile and nociceptive) almost immediately after birth (Friede and Samorajski, 1968; Fitzgerald, 1985).

Accurate classification allows further examination of developmental differences in peripheral neuronal RF characteristics otherwise not possible. Previous studies have shown that developmental differences exist with respect to the size of the RF of the glabrous skin of the paw in rat, with RF size increasing with decreasing postnatal age (Torsney and Fitzgerald, 2002; Fitzgerald, 1985; Ririe et al., 2008). In these studies RF was determined from the spinal cord in wide dynamic range (WDR) neurons which are second order neurons receiving input from multiple primary afferent neurons. Therefore the RF measured in this way is an integrated response at the level of the spinal cord. In the current study, RF size and character of the primary afferent was found to be specific to the peripheral afferent neuron subtype. Relative size of the RF was larger in the neurons from the younger animals for both LTMR and HTMR, but the character of the HTMR in the older animals was more distinct and more likely to be spot-like. This larger and more diffuse RF of the peripheral neuron from the younger P7 suggests that the RF size is not solely regulated at the spinal cord level, but is an intrinsic property of the peripheral afferent subtype during development (depending on mechanical threshold responses; LTMR and HTMR).

Neuronal subtypes retain and develop a set of basic properties that are immature but persist into adulthood, increasing the developmental contrast for neuronal modalities. The changes in the RF size and character in the peripheral sensory neuron from infant to juvenile, RF being reduced by one order of magnitude to a typical high threshold single-spot configuration, is similar to other rodents under similar conditions (Boada and Woodbury, 2007; 2008; Boada et al., 2010). This process is not homogenous in the extremity and depends on the area (toe vs sole) skin type innervated (Boada et al., 2010). Compared to the

sole of the foot, RF areas in the toes show that tactile receptors are more mature, with nociceptors even closer to their adult status in the young (smaller single point RF). This fundamental information of the RF during development will be valuable in understanding the impact of early injury in the peripheral afferent and its contribution to changes measured in the DH of the spinal cord. This will be valuable in understanding effects of injury at critical periods of development on circuit establishment in the spinal cord. It will also help understand the impact of injury on altered sensory input from changes in the RF in different neuron populations.

5. Conclusion

This study provides fundamental knowledge of differences in peripheral mechanosensitive afferent characteristics during development. The level of dependency of maturation of mechanoreceptors from early activation or how early damage in a RF affects the maturation process is unclear. The effect that differences in CV and anatomic location of signal transmission in the DH have on normal circuit development will be valuable. Finally effects of injury or accelerated noxious input on peripheral nerve development, DH circuitry and higher levels of sensory integration will be of considerable importance.

Acknowledgments

Supported by National Institutes of Health Grants GM72105 and NS57594 (Bethesda, Maryland)

References

Albers KM, Woodbury CJ, Ritter AM, Davis BM, Koerber HR. Glial cell-line-derived neurotrophic factor expression in skin alters the mechanical sensitivity of cutaneous nociceptors. J. Neurosci. 2006; 26:2981–2990. [PubMed: 16540576]

Beggs S, Torsney C, Drew LJ, Fitzgerald M. The postnatal reorganization of primary afferent input and dorsal horn cell receptive fields in the rat spinal cord is an activity-dependent process. Eur. J. Neurosci. 2002; 16:1249–1258. [PubMed: 12405985]

Benn SC, Costigan M, Tate S, Fitzgerald M, Woolf CJ. Developmental expression of the TTX-resistant voltage-gated sodium channels Nav1.8 (SNS) and Nav1.9 (SNS2) in primary sensory neurons. J. Neurosci. 2001; 21:6077–6085. [PubMed: 11487631]

Bessou P, Perl ER. Response of cutaneous sensory units with unmyelinated fibers to noxious stimuli. J. Neurophysiol. 1969; 32:1025–1043. [PubMed: 5347705]

Boada MD, Houle TT, Eisenach JC, Ririe DG. Differing neurophysiologic mechanosensory input from glabrous and hairy skin in juvenile rats. J. Neurophysiol. 2010; 104:3568–3575. [PubMed: 20926608]

Boada MD, Woodbury CJ. Physiological properties of mouse skin sensory neurons recorded intracellularly in vivo: temperature effects on somal membrane properties. J. Neurophysiol. 2007; 98:668–680. [PubMed: 17537905]

Boada MD, Woodbury CJ. Myelinated skin sensory neurons project extensively throughout adult mouse substantia gelatinosa. J. Neurosci. 2008; 28:2006–2014. [PubMed: 18305235]

Burgess PR, Perl ER. Myelinated afferent fibres responding specifically to noxious stimulation of the skin. J. Physiol. 1967; 190:541–562. [PubMed: 6051786]

Campbell, JN.; Raja, SN.; Cohen, SH.; Manning, DC.; Meyer, RA. Peripheral neuronal mechanisms of nociception. In: Wall, PD.; Melzack, R., editors. Textbook of Pain. Churchill Livingstone; Edinburgh, London: 1989. p. 22-45.

Coggeshall RE, Jennings EA, Fitzgerald M. Evidence that large myelinated primary afferent fibers make synaptic contacts in lamina II of neonatal rats. Brain Res. Dev. Brain Res. 1996; 92:81–90.

Djouhri L, Bleazard L, Lawson SN. Association of somatic action potential shape with sensory receptive properties in guinea-pig dorsal root ganglion neurones. J. Physiol. 1998; 513:857–872. [PubMed: 9824723]

Fang X, McMullan S, Lawson SN, Djouhri L. Electrophysiological differences between nociceptive and non-nociceptive dorsal root ganglion neurones in the rat in vivo. J. Physiol. 2005; 565:927–943. [PubMed: 15831536]

Fitzgerald M. The post-natal development of cutaneous afferent fibre input and receptive field organization in the rat dorsal horn. J. Physiol. 1985; 364:1–18. [PubMed: 4032293]

Fitzgerald M. Cutaneous primary afferent properties in the hind limb of the neonatal rat. J. Physiol. 1987; 383:79–92. [PubMed: 3656143]

Fitzgerald M. The development of activity evoked by fine diameter cutaneous fibres in the spinal cord of the newborn rat. Neurosci. Lett. 1988; 86:161–166. [PubMed: 3368118]

Fitzgerald M, Butcher T, Shortland P. Developmental changes in the laminar termination of A fibre cutaneous sensory afferents in the rat spinal cord dorsal horn. J. Comp. Neurol. 1994; 348:225–233. [PubMed: 7814689]

Fitzgerald M, Gibson S. The postnatal physiological and neurochemical development of peripheral sensory C fibres. Neuroscience. 1984; 13:933–944. [PubMed: 6084831]

Friede RL, Samorajski T. Myelin formation in the sciatic nerve of the rat. A quantitative electron microscopic, histochemical and radioautographic study. J. Neuropathol. Exp. Neurol. 1968; 27:546–570. [PubMed: 4879906]

Fulton BP. Postnatal changes in conduction velocity and soma action potential parameters of rat dorsal root ganglion neurones. Neurosci. Lett. 1987; 73:125–130. [PubMed: 3822244]

Harper AA, Lawson SN. Conduction velocity is related to morphological cell type in rat dorsal root ganglion neurones. J. Physiol. 1985; 359:31–46. [PubMed: 3999040]

Harper AA, Lawson SN. Electrical properties of rat dorsal root ganglion neurones with different peripheral nerve conduction velocities. J. Physiol. 1985; 359:47–63. [PubMed: 2987489]

Klein JP, Tendi EA, Dib-Hajj SD, Fields RD, Waxman SG. Patterned electrical activity modulates sodium channel expression in sensory neurons. J. Neurosci. Res. 2003; 74:192–198. [PubMed: 14515348]

Lawson SN. Phenotype and function of somatic primary afferent nociceptive neurones with C-, Adelta- or Aalpha/beta-fibres. Exp. Physiol. 2002; 87:239–244. [PubMed: 11856969]

Li J, Baccei ML. Excitatory synapses in the rat superficial dorsal horn are strengthened following peripheral inflammation during early postnatal development. Pain. 2009; 143:56–64. [PubMed: 19249156]

Li J, Walker SM, Fitzgerald M, Baccei ML. Activity-dependent modulation of glutamatergic signaling in the developing rat dorsal horn by early tissue injury. J. Neurophysiol. 2009; 102:2208–2219. [PubMed: 19675290]

Light, AR.; Perl, ER. Peripheral sensory systems. In: Dyck, PJ.; Thomas, PK.; Griffin, JW.; Low, PA., editors. Peripheral Neuropathy. W.B. Saunders; Philadelphia, PA: 1993. p. 149-165.

Lu J, Zhou XF, Rush RA. Small primary sensory neurons innervating epidermis and viscera display differential phenotype in the adult rat. Neurosci. Res. 2001; 41:355–363. [PubMed: 11755222]

Perl, ER. Function of dorsal root ganglion neurons: an overview. In: Scott, SA., editor. Sensory Neurons: Diversity, Development and Plasticity. Oxford University Press; New York: 1992. p. 3-23.

Ririe DG, Bremner LR, Fitzgerald M. Comparison of the immediate effects of surgical incision on dorsal horn neuronal receptive field size and responses during postnatal development. Anesthesiology. 2008; 109:698–706. [PubMed: 18813050]

Ririe DG, Liu B, Clayton B, Tong C, Eisenach JC. Electrophysiologic characteristics of large neurons in dorsal root ganglia during development and after hind paw incision in the rat. Anesthesiology. 2008; 109:111–117. [PubMed: 18580180]

Rowe MJ. Development of mammalian somatosensory pathways. Trends. Neurosci. 1982; 5:408–411.

Torsney C, Fitzgerald M. Age-dependent effects of peripheral inflammation on the electrophysiological properties of neonatal rat dorsal horn neurons. J. Neurophysiol. 2002; 87:1311–1317. [PubMed: 11877505]

Woodbury CJ, Koerber HR. Widespread projections from myelinated nociceptors throughout the substantia gelatinosa provide novel insights into neonatal hypersensitivity. J. Neurosci. 2003; 23:601–610. [PubMed: 12533620]

Woolf CJ, Fitzgerald M. The properties of neurones recorded in the superficial dorsal horn of the rat spinal cord. J. Comp. Neurol. 1983; 221:313–328. [PubMed: 6197429]

Highlights

- Peripheral receptive field size is larger in the young and is a property of low and high threshold neurons.
- Conduction velocity is inadequate for classification of mechanosensitive neurons early in development.
- Combining partially conserved neuron properties makes classification of peripheral afferent fibers possible in early development.
- This knowledge will enable understanding of noxious input at critical periods early in postnatal life.

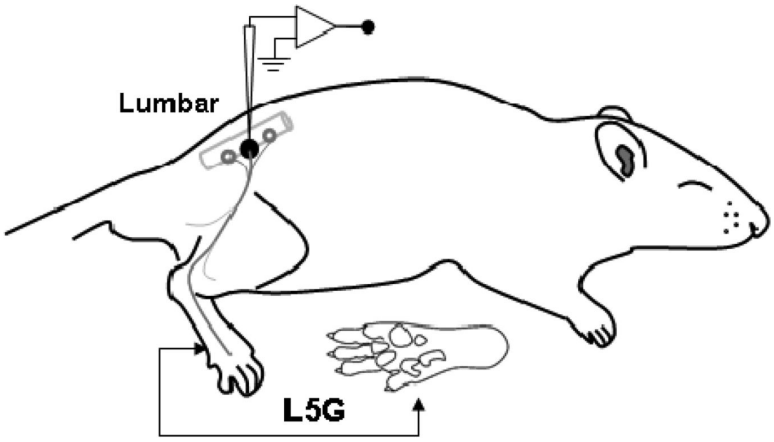

Figure 1.
Schematic diagram of the *in vivo* rat L5 preparation (lateral view).

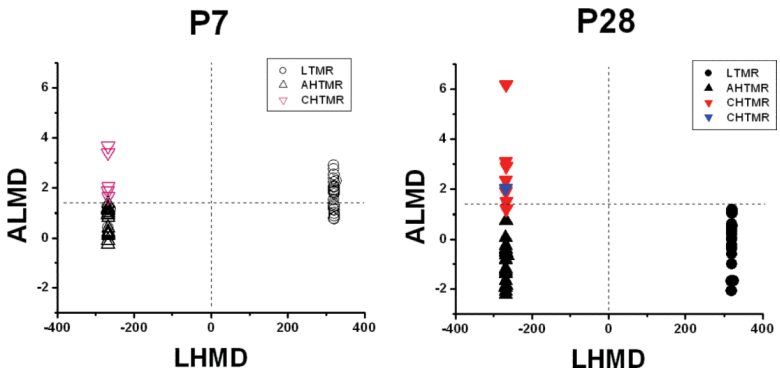

Figure 2.

Classification of neurons using canonical correlation. The model was developed for the P28 neurons with 2 canonical variates, the low-high mechanical discriminator (LHMD) and the A-C mechanical discriminator (ACMD). The P28 graph is the application of the model to P28 neurons (● LTMR, ▲ AHTMR, CHTMR ▼predicted, ▼predicted incorrectly). The P7 graph is the application of the model to the neurons at P7 (○ LTMR, △ AHTMR, CHTMR △). The separation of the LTMR and the HTMR is shown with the dashed line at zero on the x-axis. The separation of the HTMR into AHTMR and CHTMR is shown by the dashed line at 1.4 on the y-axis.

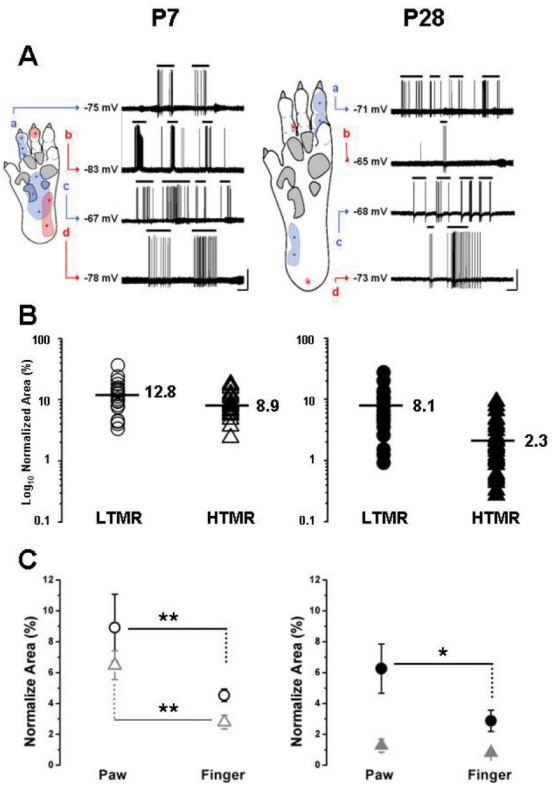

Figure 3.

A. Representative cellular RFs diagrams on the animals feet at both ages (P7 and P28), represented with the areas of maximal sensibility (threshold response) (color dots) and the absolute area of their RF at suprathreshold intensities (colored area). All cells are also shown with their responses and Resting membrane potential (Em) (LTMR afferents: blue a and c; HTMR afferents: red b and d).

B. Developmental differences in normalized RF for LTMR and HTMR for neurons at P7 and P28 (P7: ○ LTMR, △ AHTMR and P28: ● LTMR, ▲ HTMR). The RF for LTMR at both P7 and P28 are significantly larger than the HTMR. LTMR and HTMR RF are also significantly larger at P7 than at P28.

C. Comparison between normalized RF areas at different functional regions of the glabrous skin of the foot (sole and fingers) at both ages (P7: ○ LTMR, △ AHTMR and P28: ● LTMR, ▲ HTMR). (*=$p<0.05$, **= $p<0.01$).

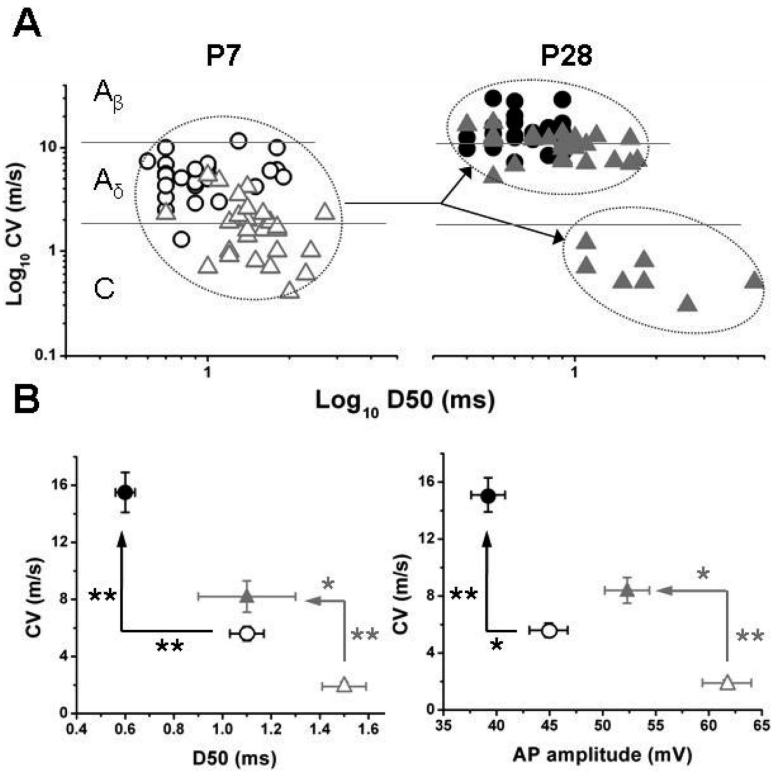

Figure 4.

A. Distribution of cellular sub-types according to conduction velocity and action potential characteristics (log10CV and log10AP duration (D50) at P7 (○ LTMR, △ HTMR) and P28 (● LTMR, ▲ HTMR). Arrows are pointing to the split in the HTMR population to fast and slow nociceptors (AHTMR and CHTMR) as observed on P28.

B. Changes on the relation between CV and two AP characteristics (duration [D50] and amplitude, respectively) on the development of the main cellular sub-types on glabrous skin. Note than both cellular subtypes show a significant increment in CV in the while their AP duration and amplitude are both reduced (*=P<0.05, **= p<0.01).

Table 1

P28 Canonical Correlation Weights and Raw Coefficients for Each Variable

Variables	LHMD	ACMD	P-value
MT	-0.56 (-0.01)	0.04 (0.01)	<0.001
CV	0.52 (-0.07)	-0.65 (-0.11)	<0.001
AP amp	-0.54 (0.01)	0.38 (0.01)	<0.001
D50	-0.38 (-0.19)	0.74 (1.76)	<0.001
AHP amp	-0.42 (0.01)	0.18 (0.07)	<0.001
AHP50	-0.45 (0.04)	-0.06 (0.14)	<0.001
Rf	0.46 (0.01)	-0.009 (0.003)	<0.001
VIB	1 (588)	-0.0008 (1.86)	<0.001

Weights of the canonical correlation coefficients are presented with the raw coefficient in parentheses. Wilkes Lambda $p<0.0001$. Canonical Correlation for LHMD=0.99 and for ACMD=0.75 (99% and 75% of the variance in the sample variables are accounted for in the two correlation variates).

Table 2

Observed P28 Neuronal Classification Accuracy with Canonical Variates

	LTMR (actual)	**AHTMR (actual)**	**CHTMR (actual)**
LTMR (predicted)	26 (100%)	0	0
AHTMR (predicted)	0	23 (96%)	1
CHTMR (predicted)	0	1	6 (86%)

Number of the total of 57 neurons from P28 animals predicted to be low threshold mechanoreceptors (LTMR), A-high threshold mechanoreceptors (AHTMR), C-high threshold mechanoreceptors (CHTMR) compared to actual classification.

Table 3

Glabrous Skin Mechanosensitive Neuron Properties from P7 and P28 Rats *In Vivo*

			Somatic Electrical Properties									Neuron Properties	
			Passive			Active							
						AP			AHP				
	Age	n	Em, mV	Ri, MΩ	τ, ms	Amplitude, mV	MRD	MRR	D50, ms	Amplitude, mV	AHP50, ms	MT, mN	CV, m/s
LTMR	P7	25	-65 (11)	111 (31)	1.9 (1.1)	45 (9)	132 (62)	-77 (28)	1.0(0.4) *†	7 (4)†	5.1 (3.3)†	0.02 (0.007-0.07)†	5.6 (2.4)*
	P28	26	-65 (7)	98 (34)	1.7 (1.1)	39(8)†	152 (63)	-81 (36)	0.7 (0.2)†	8 (2)†	5.4 (2.7)†	0.04 (0.007-0.07)†	15.1 (5.9)†
HTMR	P7	26	-60 (12)	126 (31)	2.4 (1.5)	62 (12)* AHTMR 60 (12) CHTMR 67(11)	124 (39)	-75 (23)	1.5 (0.5)≠ AHTMR 1.4 (0.4) CHTMR 2.1 (0.6)	10 (4)	9.9 (3.8)	15 (0.16-98)	1.9 (1.3)* AHTMR 2.1 (1.3) CHTMR 1.1(0.7)
	P28	31	-64 (12)	117 (39)	1.8 (1.1)	52 (11)≠ AHTMR 50 (11) CHTMR 61 (12)	150 (76)	-78 (36)	1.2 (0.8)≠ AHTMR 0.9 (0.4) CHTMR 2.1 (1.2)	11 (4)	9.0 (4.2)	15 (0.39-98)	8.5 (5.1)† AHTMR 10.7 (3.2)≠ CHTMR 0.6 (0.3)

Numbers are presented as means with standard deviation in parentheses, except for MT which are medians and ranges.

LTMR=Tactile=low threshold mechanoreceptor, HTMR=high threshold mechanoreceptor, AHTMR=A-fiber HTMR and CHTMR=C-fiber HTMR. Postnatal day 7 rat=P7, postnatal day 28 rat=P28. Symbols:

* significant difference between the P7 and P28 LTMR or HTMR

† significant difference between the LTMR and the HTMR of P7 or P28

≠ significant difference between the AHTMR and CHTMR.